BBA - Biomembranes 1862 (2020) 183333

Contents lists available at ScienceDirect

BBA - Biomembranes

journal homepage: www.elsevier.com/locate/bbamem

Membrane proteins in magnetically aligned phospholipid polymer discs for solid-state NMR spectroscopy

Sang Ho Park[a], Jiaqian Wu[a], Yong Yao[b], Chandan Singh[b,1], Ye Tian[b], Francesca M. Marassi[b], Stanley J. Opella[a,*]

[a] University of California San Diego, La Jolla, CA, USA
[b] Sanford Burnham Prebys Medical Discovery Institute, La Jolla, CA, USA

ARTICLE INFO

Keywords:
Membrane proteins
Solid-state NMR
Macrodisc
SMA
SMALP

ABSTRACT

Well-hydrated phospholipid bilayers provide a near-native environment for membrane proteins. They enable the preparation of chemically-defined samples suitable for NMR and other spectroscopic experiments that reveal the structure, dynamics, and functional interactions of the proteins at atomic resolution. The synthetic polymer styrene maleic acid (SMA) can be used to prepare detergent-free samples that form macrodiscs with diameters greater than 30 nm at room temperature, and spontaneously align in the magnetic field of an NMR spectrometer at temperatures above 35 °C. Here we show that magnetically aligned macrodiscs are particularly well suited for solid-state NMR experiments of membrane proteins because the SMA-lipid assembly both immobilizes the embedded protein and provides uniaxial order for oriented sample (OS) solid-state NMR studies. We show that aligned macrodiscs incorporating four different membrane proteins with a wide range of sizes and topological complexity yield high-resolution OS solid-state NMR spectra. The work is dedicated to Michelle Auger who made key contributions to the field of membrane and membrane protein biophysics.

1. Introduction

Membrane proteins and their surrounding lipids have co-evolved to provide many of the unique and specific functions that constitute cellular life [1]. The physically anisotropic and chemically heterogeneous environment of the lipid bilayer influences membrane protein structures, dynamics and functions [2] and highlights the importance of performing structural studies on entire protein-lipid assemblies, near physiological conditions of temperature, pH and hydration.

Nuclear magnetic resonance (NMR) is compatible with these samples [3,4]. NMR signals provide accurate structural restraints, offer information about protein and lipid dynamics, and serve as sensitive probes of intermolecular and ligand binding events that enable structure-activity correlations to be established [5]. While solution NMR studies are primarily limited to membrane proteins solubilized in detergent micelles or small detergent-free lipid nanodiscs [6] that have short correlation times [7], solid-state NMR extends the methodology to many types of lipid bilayer samples, not just those that reorient rapidly in solution. Solid-state NMR has played a central role in shaping our current understanding of the structures and dynamics of lipids and membrane proteins, and their interactions in the complexes that constitute biological membranes [8–16]. Notably, early experiments by Michelle Auger and her coworkers were instrumental for characterizing phospholipid and glycolipid dynamics [17,18]. Importantly, they set the stage for later studies from her laboratory that provided a wealth of critical insights into the mechanisms of action of membrane-associated antibiotic peptides [19–21].

Solid-state NMR methods based on measuring the influence of immobilization and uniaxial alignment on peptides and proteins in oriented samples [21–23] are particularly useful for resolving and assigning resonances in the spectra of $^{15}N/^{13}C$ double-labeled proteins. The frequencies of single-line resonance and splittings of doublets provide powerful, angle-dependent restraints for structure determination. Oriented sample (OS) solid-state NMR relies on the preparation of planar lipid bilayer samples where the axis normal to the membrane plane aligns in a unique orientation, parallel or perpendicular to the field of the direction of the magnetic field.

Protein-containing aligned phospholipid bilayers serve as excellent membrane mimics for biophysical studies. These samples can be prepared by spreading phospholipid bilayers on hydrated glass surfaces, or

* Corresponding author.
E-mail address: sopella@ucsd.edu (S.J. Opella).
[1] Present address: Department of Biochemistry, Institute of Science, Banaras Hindu University (BHU), Varanasi, Pin-221005, India.

https://doi.org/10.1016/j.bbamem.2020.183333
Received 27 February 2020; Received in revised form 22 April 2020; Accepted 27 April 2020
Available online 01 May 2020

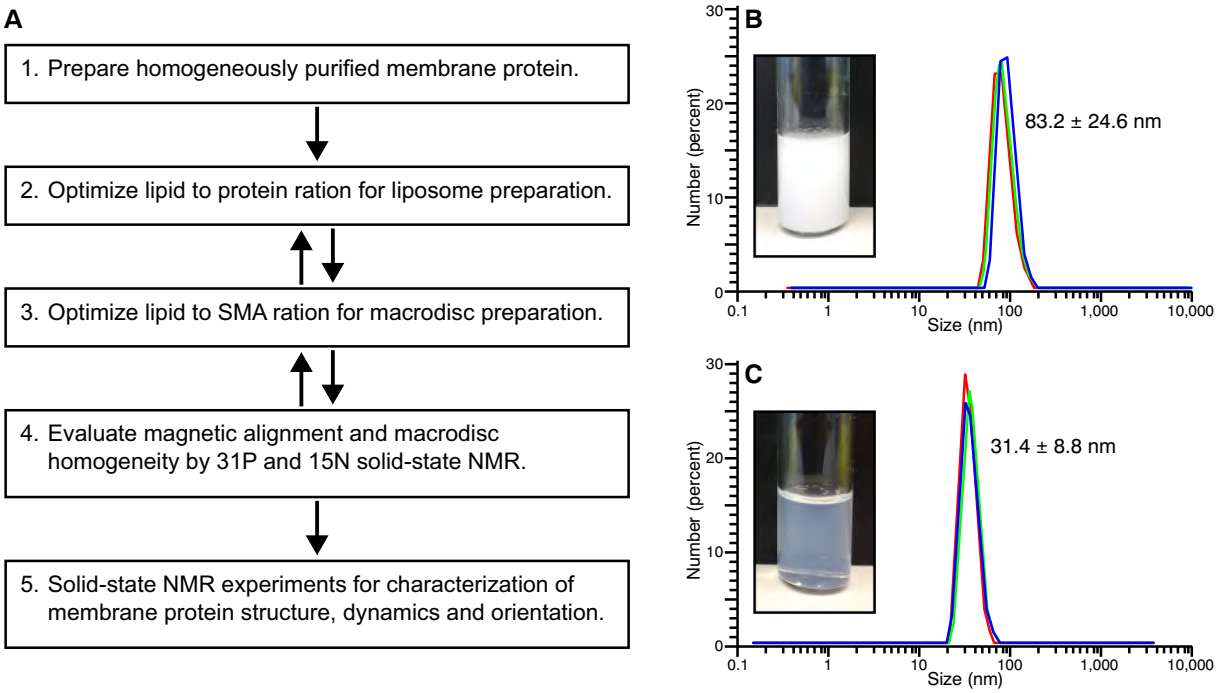

Fig. 1. Preparation of membrane proteins in magnetically aligned macrodiscs and size characterization of SMA macrodiscs. (A) Steps 2–4 are interdependent (double arrows) and require optimization. (B, C) Dynamic light scattering profiles of macrodisc size distribution versus scattering number for (B) DMPC liposomes (83.2 ± 24.6 nm) or (C) DMPC/SMA(3:1) (10/3, w/w) SMA macrodiscs (31.4 ± 8.8 nm). Different colors represent three independent measurements made for each sample. These protein-free samples are representative of protein-loaded samples. Inset images illustrate the transition to a translucent preparation that is a hallmark of macrodisc formation. DLS experiments were performed at 25 °C. The lipid concentration was 1% (w/v).

by exploiting the inherent magnetic anisotropy susceptibility of the lipids in bilayers. Both types of samples have been used successfully to determine membrane protein structures with high accuracy and precision [21–23]. The preparation of glass-aligned bilayer samples, however, remains challenging, and bicelle samples require detergents which have the potential of altering protein structure and function.

The development of nanodiscs [6] relies on forming patches of phospholipid bilayer stabilized by two copies of helical amphiphilic membrane scaffold protein (MSP). These small 6–10 nm diameter assemblies are suitable for solution NMR studies of some membrane proteins [7], but reorient too rapidly for solid-state NMR studies. Previously, we demonstrated that versions with larger diameters (macrodiscs), that are suitable for solid-state NMR, may be prepared by substituting MSP with a 14-residue amphipathic peptide at a high lipid to peptide ratio [24]. Macrodiscs offer several advantages for solid-state NMR studies: the embedded proteins experience less lateral pressure and crowding from the surrounding lipids; the assemblies are sufficiently large to immobilize their associated proteins on the NMR timescales; and finally, macrodiscs align spontaneously in the magnetic field, yielding high-resolution NMR spectra of their associated proteins. The latest version of macrodiscs described here is based on the use of styrene maleic acid (SMA) copolymers and offers several advantages. Synthetic polymers replace amphipathic polypeptides at the rim of the phospholipid bilayer discs. Importantly, this eliminates the need for detergent molecules during macrodisc formation from proteoliposomes.

SMA copolymers with alternating hydrophobic (styrene) and hydrophilic (maleic acid) moieties, have been used successfully to extract membrane proteins from their native membranes [25–31], or to solubilize artificial proteoliposomes into discrete circular lipid bilayer assemblies of defined diameter [25,32–34]. Several membrane proteins have been studied in SMA preparations [25,29,32,35], and analogous polymers with greater pH stability and decreased susceptibility to divalent metal cations are being developed [36–39].

While the size of SMA discs may be tuned by altering the lipid to SMA ratio, and smaller SMA nanodiscs offer potential for solution NMR applications [40–42], their relatively large diameters (~10 nm) and heterogeneous size distributions result in significantly broader NMR linewidths and poorly resolved spectra compared to those obtained with MSP nanodiscs [7]. On the other hand, we have shown that SMA macrodiscs with disc diameters in the range of 25–45 nm can align spontaneously in the magnetic field and are well suited for OS solid-state NMR studies of membrane proteins [34]. We also demonstrated that these samples have the important advantage that they can be flipped between orientations with the membrane normal parallel or perpendicular to the field by adding lanthanide ions such as Tm^{3+}, and therefore, provide a powerful approach for enhancing spectral resolution, obtaining resonance assignments, and measuring accurate orientation-dependent restraints for structure determination [43,44]. Previous demonstrations of magnetically aligned SMA macrodiscs focused on solid-state NMR spectra of a 46-residue membrane protein with a single transmembrane helix, the major coat protein from Pf1 bacteriophage [34]. Here we describe preparations that enable larger and more complex membrane proteins to be incorporated in SMA macrodiscs for OS solid-state NMR. The results build upon a large body of research on aligned lipid bilayers that includes seminal work by Michelle Auger and her laboratory [21].

2. Materials and methods

2.1. Materials

1,2-Dimyristoyl-sn-glycero-3-phosphocholine (DMPC) and 1,2-Dimyristoyl-sn-glycero-3-phosphorylglycerol sodium salt (DMPG) were purchased from Anatrace (www.anatrace.com). SMA(3:1), a pre-hydrolyzed styrene-maleic acid copolymer with a 3/1 ratio of styrene to maleic acid, was provided by Polyscope (www.polyscope.eu).

Table 1
Sample conditions of protein-containing SMA macrodiscs for OS solid-state NMR experiments.

Protein	DMPC/DMPG (molar)	Lipid/protein (molar)	Buffer
Pf1 coat	1/1	101	20 mM HEPES, pH 8
MerFt	1/1	138	20 mM HEPES, pH 7.4
Ail	4/1	100	10 mM NaPi, pH 7
CXCR1	4/1	600	20 mM HEPES, pH 7.4

2.2. SMA macrodisc preparation

The preparation of protein-containing SMA macrodiscs for OS solid-state NMR studies is outlined in Fig. 1A and the final sample condition are listed in Table 1. First, pure and homogeneous membrane proteins were prepared by final HPLC purification in either trifluoroethanol/water organic solvent (Pf1 coat protein and MerFt) or size-exclusion chromatography in detergent (Ail and CXCR1). Next, the lipid to protein ratio and lipid composition was optimized to obtain stable homogeneous proteoliposomes. To obtain maximum sensitivity in the protein NMR spectra, the protein concentration was gradually increased while keeping the lipid concentration constant, and the protein aggregation was monitored by SDS-PAGE. This step is important for successful macrodisc formation. The final samples contained DMPC/DMPG = 1/1 (molar) for Pf1 coat protein and MerFt, or DMPC/DMPG = 4/1 (molar) for Ail and CXCR1). Third, the lipid to SMA ratio was optimized by titrating SMA into proteoliposomes to obtain homogeneously translucent macrodiscs (Fig. 2B, C). The final ratio of lipid/SMA was between 10/2 and 10/30 (by weight). The lipid concentration of the final macrodics was adjusted between 10% and 20% (w/v). Fourth, the magnetic alignment and homogeneity of protein-containing macrodiscs was evaluated by ^{31}P and ^{15}N solid-state NMR for the lipids and proteins, respectively. Finally, ^{1}H/^{15}N 1D and 2D NMR experiments were performed to characterize membrane protein structure, dynamics, and orientation.

Dynamic light scattering (DLS) experiments (Fig. 1B, C) were performed using a Malvern Instruments Zetasizer Nano-ZS, at 25 °C, with a backscatter angle of 173°. The data were fitted using the protein analysis model for data processing. DMPC liposomes and DMPC/SMA(3:1) macrodiscs had lipid concentrations of 1% (w/v).

2.3. Protein preparation

Uniformly ^{15}N-labeled major coat protein from Pf1 bacteriophage was prepared and purified as described previously [24,45]. Briefly, 2 mg of HPLC-purified and lyophilized protein was dissolved in 1 mL of neat trifluoroethanol and mixed with 30 mg of DMPC/DMPG (1/1 molar) dissolved in 1 mL of trifluoroethanol/chloroform (1/1, v/v). The organic solvent was then evaporated under a stream of nitrogen gas to obtain a thin, transparent protein/lipid film, which was placed under high vacuum overnight. Homogeneous proteoliposomes were obtained by suspending the protein/lipid film in 2 mL of 20 mM HEPES buffer, pH 8.0 with multiple heat (40 °C) and cold (on ice) cycles.

Uniformly ^{15}N-labeled truncated bacterial mercury transporter MerFt was prepared and purified as described previously [46,48]. Briefly, 2 mg of HPLC-purified and lyophilized protein was dissolved in 1 mL of trifluoroethanol/trifluoracetic acid (99.9/0.1 by vol.) and filtered through 0.2 μm polytetrafluoroethylene syringe filter to remove insoluble aggregates. The protein solution was then mixed with 30 mg of DMPC/DMPG (1/1, molar) dissolved in 1 mL trifluoroethanol/chloroform (1/1, v/v). The organic solvent was then evaporated under a stream of nitrogen gas to obtain a thin, transparent protein-lipid film, which was placed under high vacuum overnight. Homogeneous proteoliposomes were obtained by dissolving the suspending the protein/lipid film in 2 mL of 20 mM HEPES buffer, pH 7.4 with multiple heat (40 °C) and cold (on ice) cycles.

Uniformly ^{15}N-labeled wild-type outer membrane protein Ail from *Yersinia pestis* was prepared and purified as described previously [49–51]. Briefly, 2 mg of lyophilized Ail was refolded in 170 mM of the detergent decylphosphocholine. Refolded Ail was mixed with 25 mg of DMPC/DMPG (4:1 molar) and dialysed against 20 mM Tris-Cl, pH 8 for 72 h to remove detergent. The resulting Ail proteoliposomes were then mixed with 3 mg SMA and submitted to several heat (42 °C) and cold (on ice) cycles to obtain homogeneously translucent macrodiscs.

Uniformly ^{15}N-labeled human chemokine receptor CXCR1 was prepared and purified as described previously [47,52]. Briefly, 3 mg of monomeric CXCR1 purified in 0.25% (w/v) dodecylphosphocholine micelles were mixed with 30 mg of DMPC/DMPG (4/1, molar) liposomes at a final volume of 3 mL of buffer solution (20 mM HEPES, 50 mM NaCl, pH 7.4) and incubated overnight at 25 °C with gentle stirring. Detergents were removed by 4000-fold dialysis (10 kDa molecular weight cutoff) against 20 mM HEPES, 50 mM NaCl, pH 7.4 buffer over the course of 3 days. The dialyzed suspension was supplemented with 30 mg of Bio-Beads SM-2 (www.bio-rad.com) and incubated for 2 h at 25 °C to remove residual detergent. Removal of Bio-Beads yielded homogeneous proteoliposomes and protein homogeneity was verified by SDS-PAGE.

2.4. Solid-state NMR experiments

One-dimensional ^{31}P NMR experiments were performed on a Bruker Avance spectrometer with a homebuilt ^{1}H/^{31}P double-resonance probe [53], at a ^{1}H resonance frequency of 700 MHz. The ^{31}P NMR spectra were obtained at 35 °C by direct single pulse excitation with a radio frequency (RF) field strength of 50 kHz, 10 ms acquisition time, 2 s recycle delay, and co-addition of 64 transients. Continuous wave ^{1}H decoupling, with RF field strength of 25 kHz, was applied during data acquisition. ^{31}P chemical shifts were externally referenced to phosphoric acid solution at 0 ppm.

Two-dimensional ^{1}H/^{15}N separated local field (SLF) NMR experiments were performed using the SAMPI4 pulse sequence [54], on a Bruker Avance III HD spectrometer with a home-built low-E ^{1}H/^{15}N double-resonance probe [55], at a ^{1}H resonance frequency of 900 MHz. Signal averaging required 64–512 transients for each of 64–128 t1 increment. The NMR data were processed using Bruker Topspin 4.0.7 and NMRPipe/NMRDraw [56]. The data were zero-filled to form a final 2048 × 2048 matrix. ^{15}N chemical shifts were externally referenced to ^{15}N labeled ammonium sulfate powder at 26.8 ppm.

2.5. Computational methods

All calculations were performed with Xplor-NIH [57,58], using the eefxPot energy function for implicit membrane solvation [59,60]. The protein coordinates were taken from the Protein data Bank (PDB) with identifiers: 2KSJ (Pf1), 2LJ2 (MerFt), 5VJ8 (Ail), and 2LNL (CXCR1), and subjected to 500 ps of minimization, followed by 100 ps of Cartesian dynamics. The thickness of the eefxPot membrane was set to 25 Å to reflect the thickness of mixed DMPC/DMPG lipid bilayers.

The ^{15}N chemical shift and ^{1}H/^{15}N dipolar coupling frequencies were calculated by fixing the axes of an axially symmetric order tensor parallel to the z axis of the eefxPot membrane, which corresponds to the membrane normal [59,60]. Two separate, tensors with different values of the magnitude (*Da*) were used to allow for differences in conformational dynamics in transmembrane helices and membrane-surface regions of the proteins. In the case of Pf1, the two-dimensional SLF spectrum (Fig. 2M) was assigned by direct comparison to the previously assigned SLF data from magnetically aligned bicelles [45], and the assigned data from SMA macrodiscs were used to restrain the dynamics. For MerFt and CXCR1, the dynamics were restrained by applying the experimental values of ^{15}N chemical shift and ^{1}H/^{15}N dipolar coupling measured previously in bicelles or liposomes [46,47]. For Ail, the

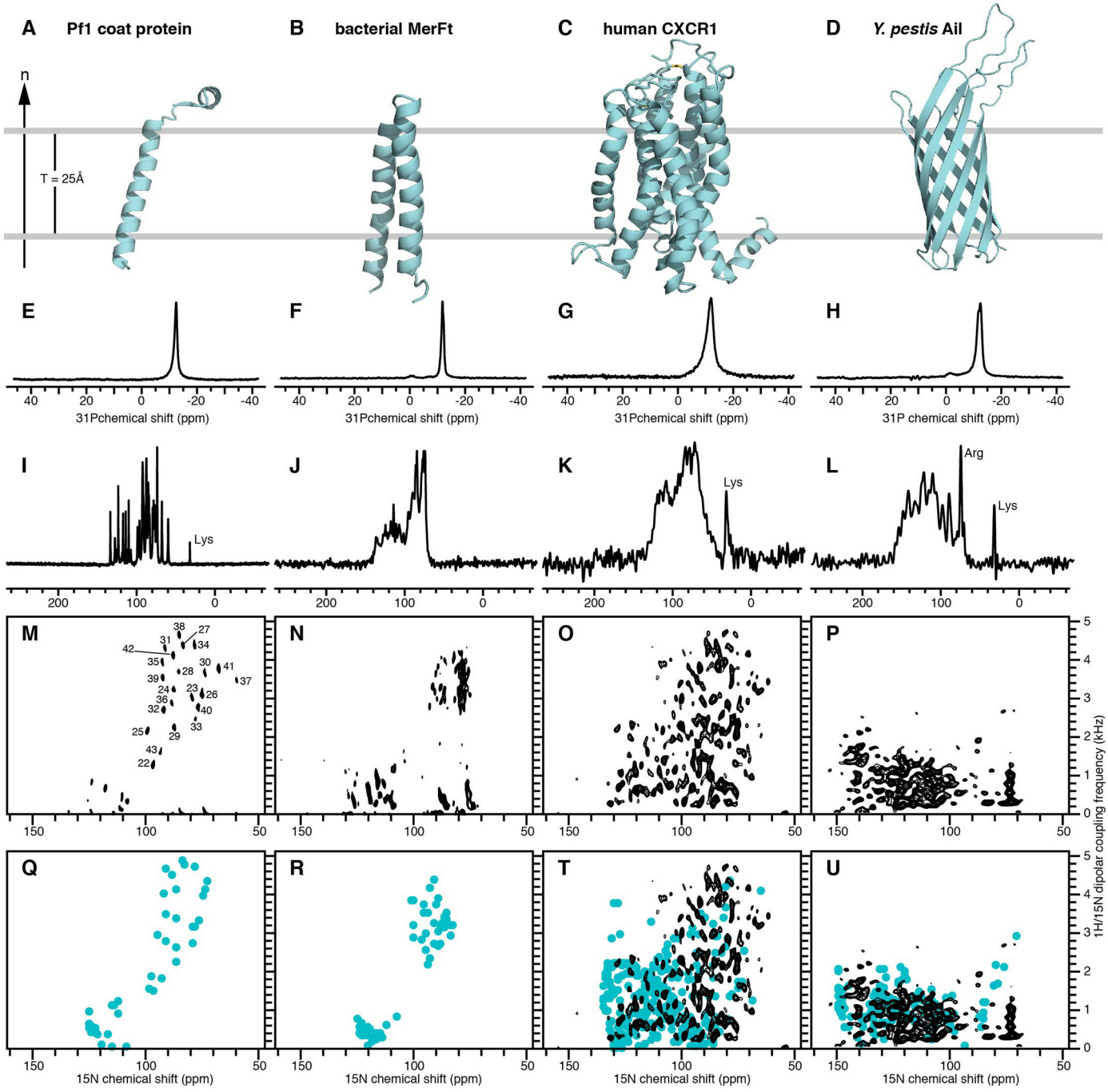

Fig. 2. Solid-state NMR spectra of four membrane proteins in magnetically aligned SMA macrodiscs. (A–D) Representations of the protein structures after 100 ps of dynamics with *eefxPot*, where the starting structures were determined by solid-state NMR (A, B, C) or solution NMR (D) in lipid bilayers: Pf1 major coat protein (PDB: 2KSJ), MerFt (PDB: 2LJ2), Ail (PDB: 5VJ8), and CXCR1 (PDB: 2LNL). The gray horizontal lines depict the membrane boundaries. The structure of pF1 was calculated with the assigned data from the SLF spectrum (M) in SMA macrodiscs. (E–H) ^{31}P NMR spectra. (I–L) ^{15}N NMR spectra. (M–P) Two-dimensional ^{1}H/^{15}N SLF spectra. The spectrum of Pf1 was assigned by comparison with the spectra from bicelles. (Q–U) Back-calculated ^{1}H/^{15}N SLF spectra derived from the membrane-embedded protein structures. Peaks from sidechains and N- and C-termini are not shown. For Pf1, the experimental SLF spectrum was assigned by direct comparison to the previously assigned SLF data from bicelles [45], and the assigned SMA data were used to restrain the dynamics for back-calculation. For MerFt and CXCR1, the dynamics were restrained by directly applying the experimental values of ^{15}N chemical shift and ^{1}H/^{15}N dipolar coupling measured previously in bicelles or liposomes [46,47]. For Ail, the dynamics were not restrained and the protein was allowed to adopt the preferred orientation dictated solely by the membrane potential of eefxPot.

dynamics were not restrained and the protein coordinates were first embedded in the implicit membrane of *eefxPot* and then allowed to adopt the preferred orientation dictated solely by the eefxPot membrane potential.

3. Results and discussion

One- and two- dimensional solid-state NMR spectra of four integral membrane proteins incorporated in SMA macrodiscs are shown in Fig. 2. The macrodiscs align with their membrane normal perpendicular to the direction of the external magnetic field. The proteins vary in size,

secondary structure, and structural complexity (Fig. 2A–D). They include: the major coat protein of Pf1 bacteriophage (46 residues, one transmembrane helix); MerFt, a truncated version of the bacterial mercury detoxification protein MerFt (60 residues, two transmembrane helices); the outer membrane protein Ail from *Yersinia pestis* (156 residues, eight-stranded β-barrel), and the human chemokine receptor CXCR1 (350 residues, seven transmembrane helices). The structures of these proteins have all been determined previously by solid-state NMR spectroscopy in other types of phospholipid bilayer samples [45–48,50,51]. Improvements in structural precision and accuracy are anticipated from determining their structures in SMA macrodiscs.

Macrodiscs are magnetically alignable lipid bilayer discs. The samples were prepared by first reconstituting each protein in proteoliposomes prepared with a mixture of DMPC and DMPG, and then adding SMA(3:1) co-polymer to form a translucent solution (Fig. 2C). Maintaining lipid to protein molar ratios > 100 is critical for the formation of liquid crystalline lipid bilayers as well as reducing the potential for forming protein-protein close contacts that lead to unwanted aggregation. Macrodisc formation was monitored by the reduction of sample turbidity at 25 °C and magnetic alignment was confirmed by the conversion of ^{31}P NMR spectra from powder patterns to single resonance lines at 35 °C.

The requirement for size homogeneity is very high in the case of solution NMR, where narrow lines rely on the preparation of small nanodiscs with very narrow size distribution in the range of 8 nm [7], as we have observed for Ail [49–51]. In the case of solid-state NMR, however, size homogeneity is not an issue, but two things are important: that the lipid bilayer membrane has a homogeneous phase and the embedded protein has a homogeneous conformation. Such phase and conformational homogeneity are completely reflected in the ^{31}P and ^{15}N solid-state NMR spectra of the magnetically aligned bilayer samples, where narrow lines reflect the homogeneity of magnetic alignment, lipid phase and protein conformation.

At 25 °C, macrodiscs have discrete diameters in the range of 32 nm, as measured by dynamic light scattering (Fig. 1C). Nevertheless, at 35 °C in the magnetic field, these macrodiscs form a magnetically aligned phase. This forms extended lipid bilayers with their membrane normal perpendicular to the magnetic field, and likely resembles the smectic phase of magnetically aligned bicelles [34].

The single line ^{31}P NMR spectra acquired at 35 °C have a chemical shift value of −13 ppm, confirming that the SMA macrodiscs align with the phospholipid membrane normal perpendicular to the applied magnetic field (Fig. 2E–H). The absence of signal near 20 ppm demonstrates a high degree of homogeneous magnetic alignment for all samples. Interestingly, the ^{31}P chemical shift frequencies reflect a higher degree of uniaxial order compared to bicelles prepared by doping phospholipid bilayers with short-chain lipids or detergents, which have axial values of the ^{31}P chemical shift in the range of −11 ppm and corresponding order parameters of 0.8–0.85, relative to the full ^{31}P axial value of −14 ppm (order parameter = 1) observed for liquid crystalline DMPC/DMPG mixtures in large vesicles with diameters > 500 nm [61]. By contrast, the −13 ppm value of the axial chemical shift of aligned macrodiscs reflects an order parameter in the range of 0.9–0.95.

Consistent with high uniaxial alignment of the SMA macrodiscs, the one-dimensional ^{15}N chemical shift spectra from the membrane embedded ^{15}N labeled proteins also display single lines (Fig. 2I–L), demonstrating that the proteins are also highly aligned. The spectra have very narrow linewidths; for example, the membrane-bound form of Pf1 coat protein has resonance linewidths of 0.3 ppm. At least twenty five ^{15}N resonances can be resolved in the one-dimensional ^{15}N spectrum of the 46-residue Pf1 coat protein in aligned SMA macrodiscs, reflecting the high degree of uniaxial symmetry of these samples. As observed for ^{31}P, the ^{15}N spectra have chemical shift frequency dispersions consistent with greater order parameters (0.9–0.95) than observed for the same proteins in bicelles.

In all cases, the absence of ^{31}P signal intensity at the isotropic frequency near −1 ppm further excludes the presence of small isotropic protein/lipid/SMA assemblies. Moreover, the absence of powder patterns in either ^{31}P or ^{15}N NMR spectra, indicates that (1) the lipids form a single homogeneous phase, and (2) the membrane-embedded proteins undergo fast rotational diffusion about the lipid bilayer normal, which is the major line narrowing mechanism for OS solid-state NMR spectroscopy.

The two-dimensional ^{1}H/^{15}N separated local field spectra from proteins in SMA macrodiscs have remarkably high resolution (Fig. 2M–P). The spectra provide two orientation-dependent frequencies (^{15}N chemical shift and ^{1}H−^{15}N dipole-dipole coupling) that correlate directly with the structure, membrane orientation, and dynamics of the protein. With one and two transmembrane helices, respectively, Pf1 and MerFt yield well-resolved spectra, while the spectrum of CXCR1 is more crowded as expected for a 350-residue protein with seven transmembrane helices. The spectra display characteristic PISA wheel patterns [62,63] from residues in transmembrane helices. Signals from the transmembrane helices populate the spectral region between 60 and 100 ppm of ^{15}N chemical shift and 3–5 kHz of ^{1}H−^{15}N dipolar coupling frequency (6–10 kHz dipolar coupling), while peaks from non-helical protein segments occur in the spectral region between 100 and 140 ppm and 0–2 kHz. By contrast, the outer membrane protein Ail folds as a transmembrane β-barrel. In this case, the overall alignment of the β-barrel amide NH bonds is parallel to both the macrodisc membrane plane and the magnetic field, and the ^{1}H/^{15}N spectrum (Fig. 2O) reflects the characteristic twisted wheel-like resonance pattern [64], with signals in the spectral region between 100 and 150 ppm (^{15}N) and 0–2 kHz (^{1}H−^{15}N).

To gain insights about the conformation and alignment of the proteins in the SMA macrodisc membranes, we performed restrained and unrestrained calculations of the SLF spectra using the Xplor-NIH eefxPot implicit membrane potential, that has been developed specifically for membrane proteins [59,60]. In the case of Pf1, the two-dimensional SLF spectrum (Fig. 2M) may be assigned by direct comparison to the previously assigned SLF data from magnetically aligned bicelles [45]. The assigned data, in turn, provide restraints for calculating the structure and integral membrane orientation of the protein in the SMA discs. The resulting structure (Fig. 2A) reflects the global position of the coat protein embedded in the SMA-corralled membrane, and the back-calculated SLF spectrum (Fig. 2Q) has very high cross-correlation with the experimental spectrum.

For MerFt and CXCR1, the greater number of resonances made direct assignment challenging. Here, the SLF spectra were calculated by restraining the Xplor-NIH eefxPot dynamics with the experimental values of ^{15}N chemical shift and ^{1}H/^{15}N dipolar coupling measured previously in bicelles for MerFt or liposomes for CXCR1 [46,47]. Finally, for Ail, there are no experimental OS-solid-state NMR data available, and the SLF spectra were back-calculated by embedding the protein coordinates in the implicit membrane of eefxPot, and allowing them to adopt a preferred membrane orientation without other restraining potentials.

While the spectra back-calculated for Pf1 and MerFt agree extremely well with the experimental spectra, the agreement is also remarkably good for CXCR1 and Ail, especially considering that the latter was obtained without restraints. Taken together, the results indicate that the overall protein conformations are not perturbed by the presence of SMA(3:1) and that the SMA macrodiscs provide a suitable membrane environment for structural studies of membrane proteins with varied conformations.

4. Conclusions

Here we demonstrated that SMA macrodiscs provide a valuable phospholipid bilayer system for OS solid-state NMR studies of membrane proteins. The samples and the NMR methods are validated by the

high resolution of the two-dimensional separated local field spectra of both α-helical and β-barrel membrane proteins. There is room for further development of SMA macrodiscs with the aim of obtaining samples that yield complete resolution and enable resonance assignments for proteins in the size range and structural complexity of CXCR1 and Ail. Further, since SMA has been shown to be capable of extracting and solubilizing membrane proteins along with their surrounding lipids directly from viable cells and microorganisms, this approach may lead to the determination of protein structures in their native environment under physiological conditions. The work is dedicated to the memory of Michelle Auger whose contributions were fundamentally important to the field of membrane and membrane protein biophysics.

Declaration of competing interest

The authors declare no conflict of interest.

Acknowledgments

We thank Thach Can for assistance with protein preparation and Greg Holland for assistance with DLS measurements. This research was supported by grants from the National Institutes of Health (GM 118186, and GM 122501) and by the Biotechnology Resource for Molecular Imaging of Proteins at UCSD supported by the National Institutes of Health (P41 EB 002031). It utilized the Cancer Center Structural Biology Resource supported by grant P30 CA030199.

References

[1] A.Y. Mulkidjanian, M.Y. Galperin, E.V. Koonin, Co-evolution of primordial membranes and membrane proteins, Trends Biochem. Sci. 34 (2009) 206–215.
[2] T.A. Cross, M. Sharma, M. Yi, H.X. Zhou, Influence of solubilizing environments on membrane protein structures, Trends Biochem. Sci. 36 (2011) 117–125.
[3] L. Banci, I. Bertini, C. Luchinat, M. Mori, NMR in structural proteomics and beyond, Prog. Nucl. Magn. Reson. Spectrosc. 56 (2010) 247–266.
[4] H.X. Zhou, T.A. Cross, Influences of membrane mimetic environments on membrane protein structures, Annu. Rev. Biophys. 42 (2013) 361–392.
[5] S.B. Shuker, P.J. Hajduk, R.P. Meadows, S.W. Fesik, Discovering high-affinity ligands for proteins: SAR by NMR, Science 274 (1996) 1531–1534.
[6] T.H. Bayburt, S.G. Sligar, Single-molecule height measurements on microsomal cytochrome P450 in nanometer-scale phospholipid bilayer disks, Proc. Natl. Acad. Sci. U. S. A. 99 (2002) 6725–6730.
[7] F. Hagn, M.L. Nasr, G. Wagner, Assembly of phospholipid nanodiscs of controlled size for structural studies of membrane proteins by NMR, Nat. Protoc. 13 (2018) 79–98.
[8] A.C. McLaughlin, P.R. Cullis, M.A. Hemminga, D.I. Hoult, G.K. Radda, G.A. Ritchie, P.J. Seeley, R.E. Richards, Application of 31P NMR to model and biological membrane systems, FEBS Lett. 57 (1975) 213–218.
[9] R.G. Griffin, Letter: observation of the effect of water on the 31P nuclear magnetic resonance spectra of dipalmitoyllecithin, J. Am. Chem. Soc. 98 (1976) 851–853.
[10] J. Seelig, Deuterium magnetic resonance: theory and application to lipid membranes, Q. Rev. Biophys. 10 (1977) 353–418.
[11] P.M. Macdonald, Deuterium NMR and the topography of surface electrostatic charge, Acc. Chem. Res. 30 (1997) 196–203.
[12] X.L. Warnet, A.A. Arnold, I. Marcotte, D.E. Warschawski, In-cell solid-state NMR: an emerging technique for the study of biological membranes, Biophys. J. 109 (2015) 2461–2466.
[13] S.J. Opella, F.M. Marassi, Applications of NMR to membrane proteins, Arch. Biochem. Biophys. 628 (2017) 92–101.
[14] T. Schubeis, T. Le Marchand, L.B. Andreas, G. Pintacuda, (1)H magic-angle spinning NMR evolves as a powerful new tool for membrane proteins, J. Magn. Reson. 287 (2018) 140–152.
[15] V. Ladizhansky, Applications of solid-state NMR to membrane proteins, Biochim. Biophys. Acta, Proteins Proteomics 1865 (2017) 1577–1586.
[16] V.S. Mandala, J.K. Williams, M. Hong, Structure and dynamics of membrane proteins from solid-state NMR, Annu. Rev. Biophys. 47 (2018) 201–222.
[17] M. Auger, Membrane structure and dynamics as viewed by solid-state NMR spectroscopy, Biophys. Chem. 68 (1997) 233–241.
[18] M. Auger, M.R. Van Calsteren, I.C. Smith, H.C. Jarrell, Glycerolipids: common features of molecular motion in bilayers, Biochemistry 29 (1990) 5815–5821.
[19] M. Ouellet, F. Otis, N. Voyer, M. Auger, Biophysical studies of the interactions between 14-mer and 21-mer model amphipathic peptides and membranes: insights on their modes of action, Biochim. Biophys. Acta 1758 (2006) 1235–1244.
[20] M. Fillion, G. Valois-Paillard, A. Lorin, M. Noel, N. Voyer, M. Auger, Membrane interactions of synthetic peptides with antimicrobial potential: effect of electrostatic interactions and amphiphilicity, Probiotics Antimicrob Proteins 7 (2015) 66–74.
[21] M. Fillion, M. Auger, Oriented samples: a tool for determining the membrane topology and the mechanism of action of cationic antimicrobial peptides by solid-state NMR, Biophys. Rev. 7 (2015) 311–320.
[22] S.J. Opella, F.M. Marassi, Structure determination of membrane proteins by NMR spectroscopy, Chem. Rev. 104 (2004) 3587–3606.
[23] T.A. Cross, V. Ekanayake, J. Paulino, A. Wright, Solid state NMR: the essential technology for helical membrane protein structural characterization, J. Magn. Reson. 239 (2014) 100–109.
[24] S.H. Park, S. Berkamp, G.A. Cook, M.K. Chan, H. Viadiu, S.J. Opella, Nanodiscs versus macrodiscs for NMR of membrane proteins, Biochemistry 50 (2011) 8983–8985.
[25] T.J. Knowles, R. Finka, C. Smith, Y.P. Lin, T. Dafforn, M. Overduin, Membrane proteins solubilized intact in lipid containing nanoparticles bounded by styrene maleic acid copolymer, J. Am. Chem. Soc. 131 (2009) 7484–7485.
[26] J.M. Dorr, M.C. Koorengevel, M. Schafer, A.V. Prokofyev, S. Scheidelaar, E.A. van der Cruijsen, T.R. Dafforn, M. Baldus, J.A. Killian, Detergent-free isolation, characterization, and functional reconstitution of a tetrameric K+ channel: the power of native nanodiscs, Proc. Natl. Acad. Sci. U. S. A. 111 (2014) 18607–18612.
[27] S. Gulati, M. Jamshad, T.J. Knowles, K.A. Morrison, R. Downing, N. Cant, R. Collins, J.B. Koenderink, R.C. Ford, M. Overduin, I.D. Kerr, T.R. Dafforn, A.J. Rothnie, Detergent-free purification of ABC (ATP-binding-cassette) transporters, Biochem. J. 461 (2014) 269–278.
[28] S.C. Lee, T.J. Knowles, V.L. Postis, M. Jamshad, R.A. Parslow, Y.P. Lin, A. Goldman, P. Sridhar, M. Overduin, S.P. Muench, T.R. Dafforn, A method for detergent-free isolation of membrane proteins in their local lipid environment, Nat. Protoc. 11 (2016) 1149–1162.
[29] C. Logez, M. Damian, C. Legros, C. Dupre, M. Guery, S. Mary, R. Wagner, C. M'Kadmi, O. Nosjean, B. Fould, J. Marie, J.A. Fehrentz, J. Martinez, G. Ferry, J.A. Boutin, J.L. Baneres, Detergent-free isolation of functional G protein-coupled receptors into nanometric lipid particles, Biochemistry 55 (2016) 38–48.
[30] C. Sun, S. Benlekbir, P. Venkatakrishnan, Y. Wang, S. Hong, J. Hosler, E. Tajkhorshid, J.L. Rubinstein, R.B. Gennis, Structure of the alternative complex III in a supercomplex with cytochrome oxidase, Nature 557 (2018) 123–126.
[31] W. Qiu, Z. Fu, G.G. Xu, R.A. Grassucci, Y. Zhang, J. Frank, W.A. Hendrickson, Y. Guo, Structure and activity of lipid bilayer within a membrane-protein transporter, Proc. Natl. Acad. Sci. U. S. A. 115 (2018) 12985–12990.
[32] J.M. Dorr, S. Scheidelaar, M.C. Koorengevel, J.J. Dominguez, M. Schafer, C.A. van Walree, J.A. Killian, The styrene-maleic acid copolymer: a versatile tool in membrane research, Eur. Biophys. J. 45 (2016) 3–21.
[33] N.L. Pollock, S.C. Lee, J.H. Patel, A.A. Gulamhussein, A.J. Rothnie, Structure and function of membrane proteins encapsulated in a polymer-bound lipid bilayer, Biochim. Biophys. Acta 1860 (2018) 809–817.
[34] J. Radoicic, S.H. Park, S.J. Opella, Macrodiscs comprising SMALPs for oriented sample solid-state NMR spectroscopy of membrane proteins, Biophys. J. 115 (2018) 22–25.
[35] R. Skrzypek, S. Iqbal, R. Callaghan, Methods of reconstitution to investigate membrane protein function, Methods 147 (2018) 126–141.
[36] A.O. Oluwole, B. Danielczak, A. Meister, J.O. Babalola, C. Vargas, S. Keller, Solubilization of membrane proteins into functional lipid-bilayer nanodiscs using a diisobutylene/maleic acid copolymer, Angew Chem Int Ed Engl 56 (2017) 1919–1924.
[37] S. Lindhoud, V. Carvalho, J.W. Pronk, M.E. Aubin-Tam, SMA-SH: modified styrene-maleic acid copolymer for functionalization of lipid nanodiscs, Biomacromolecules 17 (2016) 1516–1522.
[38] M.C. Fiori, Y. Jiang, G.A. Altenberg, H. Liang, Polymer-encased nanodiscs with improved buffer compatibility, Sci. Rep. 7 (2017) 7432.
[39] V. Schmidt, J.N. Sturgis, Modifying styrene-maleic acid co-polymer for studying lipid nanodiscs, Biochim. Biophys. Acta 1860 (2018) 777–783.
[40] C. Vargas, R.C. Arenas, E. Frotscher, S. Keller, Nanoparticle self-assembly in mixtures of phospholipids with styrene/maleic acid copolymers or fluorinated surfactants, Nanoscale 7 (2015) 20685–20696.
[41] R. Zhang, I.D. Sahu, L. Liu, A. Osatuke, R.G. Comer, C. Dabney-Smith, G.A. Lorigan, Characterizing the structure of lipodisq nanoparticles for membrane protein spectroscopic studies, Biochim. Biophys. Acta 1848 (2015) 329–333.
[42] R. Puthenveetil, K. Nguyen, O. Vinogradova, Nanodiscs and solution NMR: preparation, application and challenges, Nanotechnol. Rev. 6 (2017) 111–126.
[43] A.A. De Angelis, S.C. Howell, S.J. Opella, Assigning solid-state NMR spectra of aligned proteins using isotropic chemical shifts, J. Magn. Reson. 183 (2006) 329–332.
[44] G.J. Lu, W.S. Son, S.J. Opella, A general assignment method for oriented sample (OS) solid-state NMR of proteins based on the correlation of resonances through heteronuclear dipolar couplings in samples aligned parallel and perpendicular to the magnetic field, J. Magn. Reson. 209 (2011) 195–206.
[45] S.H. Park, F.M. Marassi, D. Black, S.J. Opella, Structure and dynamics of the membrane-bound form of Pf1 coat protein: implications of structural rearrangement for virus assembly, Biophys. J. 99 (2010) 1465–1474.
[46] B.B. Das, H.J. Nothnagel, G.J. Lu, W.S. Son, Y. Tian, F.M. Marassi, S.J. Opella, Structure determination of a membrane protein in proteoliposomes, J. Am. Chem. Soc. 134 (2012) 2047–2056.
[47] S.H. Park, B.B. Das, F. Casagrande, Y. Tian, H.J. Nothnagel, M. Chu, H. Kiefer, K. Maier, A.A. De Angelis, F.M. Marassi, S.J. Opella, Structure of the chemokine receptor CXCR1 in phospholipid bilayers, Nature 491 (2012) 779–783.
[48] A.A. De Angelis, S.C. Howell, A.A. Nevzorov, S.J. Opella, Structure determination of a membrane protein with two trans-membrane helices in aligned phospholipid bicelles by solid-state NMR spectroscopy, J. Am. Chem. Soc. 128 (2006) 12256–12267.

[49] Y. Ding, L.M. Fujimoto, Y. Yao, G.V. Plano, F.M. Marassi, Influence of the lipid membrane environment on structure and activity of the outer membrane protein Ail from Yersinia pestis, Biochim. Biophys. Acta 1848 (2015) 712–720.
[50] S.K. Dutta, Y. Yao, F.M. Marassi, Structural insights into the Yersinia pestis outer membrane protein ail in lipid bilayers, J. Phys. Chem. B 121 (2017) 7561–7570.
[51] Y. Yao, S.K. Dutta, S.H. Park, R. Rai, L.M. Fujimoto, A.A. Bobkov, S.J. Opella, F.M. Marassi, High resolution solid-state NMR spectroscopy of the Yersinia pestis outer membrane protein ail in lipid membranes, J. Biomol. NMR 67 (2017) 179–190.
[52] S.H. Park, F. Casagrande, M. Chu, K. Maier, H. Kiefer, S.J. Opella, Optimization of purification and refolding of the human chemokine receptor CXCR1 improves the stability of proteoliposomes for structure determination, Biochim. Biophys. Acta 1818 (2012) 584–591.
[53] C.V. Grant, S.L. Sit, A.A. De Angelis, K.S. Khuong, C.H. Wu, L.A. Plesniak, S.J. Opella, An efficient (1)H/(31)P double-resonance solid-state NMR probe that utilizes a scroll coil, J. Magn. Reson. 188 (2007) 279–284.
[54] A.A. Nevzorov, S.J. Opella, Selective averaging for high-resolution solid-state NMR spectroscopy of aligned samples, J. Magn. Reson. 185 (2007) 59–70.
[55] C.V. Grant, C.H. Wu, S.J. Opella, Probes for high field solid-state NMR of lossy biological samples, J. Magn. Reson. 204 (2010) 180–188.
[56] F. Delaglio, S. Grzesiek, G.W. Vuister, G. Zhu, J. Pfeifer, A. Bax, NMRPipe: a multidimensional spectral processing system based on UNIX pipes, J. Biomol. NMR 6 (1995) 277–293.
[57] C.D. Schwieters, J.J. Kuszewski, N. Tjandra, G.M. Clore, The Xplor-NIH NMR molecular structure determination package, J. Magn. Reson. 160 (2003) 65–73.
[58] C.D. Schwieters, J.J. Kuszewski, G. Marius Clore, Using Xplor ÄìNIH for NMR molecular structure determination, Prog. Nucl. Magn. Reson. Spectrosc. 48 (2006) 47–62.
[59] Y. Tian, C.D. Schwieters, S.J. Opella, F.M. Marassi, A practical implicit membrane potential for NMR structure calculations of membrane proteins, Biophys. J. 109 (2015) 574–585.
[60] Y. Tian, C.D. Schwieters, S.J. Opella, F.M. Marassi, High quality NMR structures: a new force field with implicit water and membrane solvation for Xplor-NIH, J. Biomol. NMR 67 (2017) 35–49.
[61] F.M. Marassi, P.M. Macdonald, Response of the headgroup of phosphatidylglycerol to membrane surface charge as studied by deuterium and phosphorus-31 nuclear magnetic resonance, Biochemistry 30 (1991) 10558–10566.
[62] F.M. Marassi, S.J. Opella, A solid-state NMR index of helical membrane protein structure and topology, J. Magn. Reson. 144 (2000) 150–155.
[63] J. Wang, J. Denny, C. Tian, S. Kim, Y. Mo, F. Kovacs, Z. Song, K. Nishimura, Z. Gan, R. Fu, J.R. Quine, T.A. Cross, Imaging membrane protein helical wheels, J. Magn. Reson. 144 (2000) 162–167.
[64] F.M. Marassi, A simple approach to membrane protein secondary structure and topology based on NMR spectroscopy, Biophys. J. 80 (2001) 994–1003.